Volume 9
Number 41
7 November 2021
Pages 14499–14948

Journal of Materials Chemistry C

Materials for optical, magnetic and electronic devices

rsc.li/materials-c

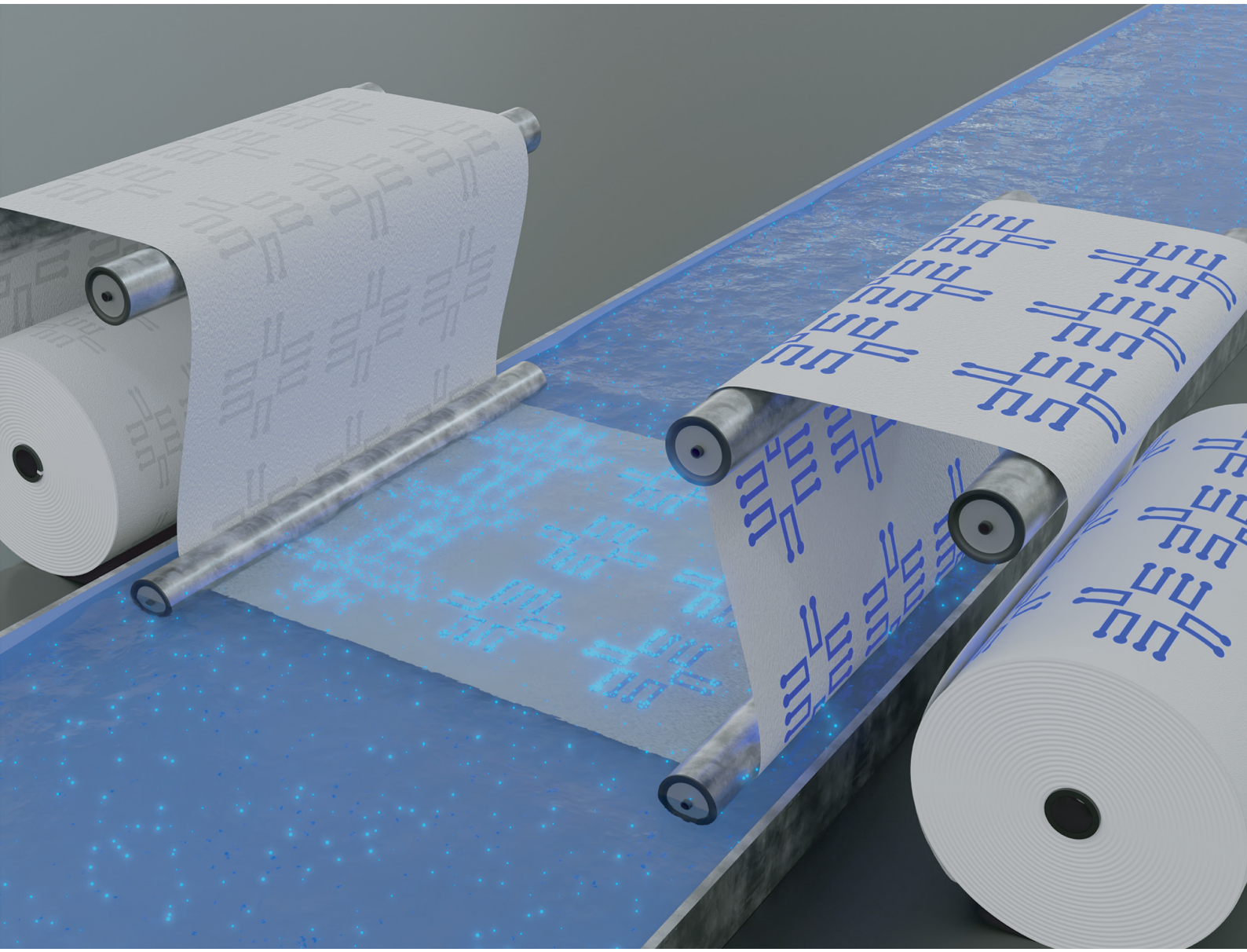

ISSN 2050-7526

ROYAL SOCIETY OF CHEMISTRY

PAPER

Mahiar M. Hamedi *et al.*

Rapid prototyping of heterostructured organic microelectronics using wax printing, filtration, and transfer

Journal of Materials Chemistry C

ROYAL SOCIETY OF CHEMISTRY

PAPER

View Article Online
View Journal | View Issue

Cite this: J. Mater. Chem. C, 2021, 9, 14596

Rapid prototyping of heterostructured organic microelectronics using wax printing, filtration, and transfer†

Liangqi Ouyang, ‡[a] Sebastian Buchmann, ‡[b] Tobias Benselfelt, [a] Chiara Musumeci, [c] Zhen Wang,[a] Shirin Khaliliazar,[a] Weiqian Tian, [a] Hailong Li, [d] Anna Herland [b] and Mahiar M. Hamedi *[a]

Received 2nd August 2021,
Accepted 2nd September 2021

DOI: 10.1039/d1tc03599a

rsc.li/materials-c

Conducting polymers are the natural choice for soft electronics. However, the main challenge is to pattern conducting polymers using a simple and rapid method to manufacture advanced devices. Filtration of conducting particle dispersions using a patterned membrane is a promising method. Here, we show the rapid prototyping of various micropatterned organic electronic heterostructures of PEDOT:PSS by inducing the formation of microscopic hydrogels, which are then filtered through membranes containing printed hydrophobic wax micropatterns. The hydrogels are retained on the un-patterned, hydrophilic regions, forming micropatterns, achieving a resolution reaching 100 μm. We further solve the problem of forming stacked devices by transferring the acidified PEDOT:PSS micropattern using the adhesive tape transfer method to form vertical heterostructures with other micropatterned electronic colloids such as CNTs, which are patterned using a similar technique. We demonstrate a number of different heterostructure devices including micro supercapacitors and organic electrochemical transistors and also demonstrate the use of acidified PEDOT:PSS microstructures in cell cultures to enable bioelectronics.

1. Introduction

Organic electronic materials, especially solution-processable conducting polymers,[1] form soft, conformal, high surface area, and conductive microstructures on various surfaces. One type of organic electronic material that has been used very successfully for various applications is the conducting polymer (CP) polyethylene(dioxythiophene):polystyrene sulfonate (PEDOT:PSS). PEDOT:PSS is an active material for making soft displays, actuators, and bio-interfaces with skin, cell, and brain contacts.[2] However, to fabricate advanced devices, PEDOT:PSS has to be micropatterned and/or stacked onto other patterned functional materials and substrates, such as metals and conductive carbon. The micropatterning of electronic heterostructures relies mainly on conventional microfabrication techniques in cleanroom environments, with multiple steps involving the spin coating of electronic materials combined with photolithography and etching steps.[3] This technique is time consuming and expensive, and the etching steps can be determinantal for some organic conductors. The residues of etchants and resists can also affect biocompatibility. It is furthermore difficult to perform photolithography on arbitrary substrates such as flexible materials. Another technique which does not involve microfabrication is printing, *e.g.*, inkjet[4] or screen printing.[5] For screen printing, inks with special rheological properties have to be developed for meshes. In inkjet printheads, the inks of colloidal particles often clog the nozzles. More problematically, it is hard to fabricate complex geometries with multiple stacks of various materials using any additive printing methods because the addition of inks from water can dissolve and alter previous layers.

3D printable PEDOT:PSS inks have been developed for the patterning of complex geometries in combination with other non-conductive printable materials, but these processes rely on time-consuming mechanisms such as cryogenic freezing, lyophilization, and dry annealing.[6]

To solve this problem, recently, we[7,8] and others[9] have developed a patterning technique where a wax printer is used

[a] Fibre and Polymer Technology (FPT) School of Engineering Sciences in Chemistry, Biotechnology and Health, KTH Royal Institute of Technology, Teknikringen 56, Stockholm, 11428, Sweden. E-mail: mahiar@kth.se
[b] Division of Micro- and Nanosystems (MST), KTH Royal Institute of Technology, Malvinas Väg 10, Stockholm, Sweden
[c] Laboratory of Organic Electronics, ITN, Linkoping University, Campus Norrkoping, SE 60221, Sweden
[d] Fysikum, Stockhohlm University, Roslagstullsbacken 21, Stockholm, Sweden

† Electronic supplementary information (ESI) available. See DOI: 10.1039/d1tc03599a

‡ Shared authors.

to pattern hydrophilic substrates, such as PVDF filtration membranes, and aqueous dispersions of colloids are subsequently vacuum filtered through the membrane; consequently, the materials are retained on the un-patterned, hydrophilic regions to form micropatterns. This method has been employed to pattern silver nanowires,[9] gold nanowires,[10] carbon nanotubes (CNTs),[11] and MXenes[8] into single-layer functional devices. However, to date, it has not been possible to pattern polymers such as PEDOT:PSS using this technique because polymers and polymer dispersions pass through filtration membranes. Furthermore, this technique does not enable the fabrication of stacked structures of different conductors and electrolytes which is necessary for advanced devices.

Here, we developed acidified PEDOT:PSS (a-PEDOT:PSS) microgels. These microgels could be retained on a wax-patterned membrane to form distinct micropatterns with a resolution reaching 100 μm. In contrast to previously reported patterned electrode arrays using a-PEDOT:PPS, the method described here does not rely on photolithography or wet etching processes and can be used to pattern flexible substrates.[12] We also post-treat the micropatterned structures with methanol to form highly water-resistant conducting a-PEDOT:PSS electrodes. We further solve the problem of forming stacked devices by transferring the a-PEDOT:PSS micropattern through tape peeling to form vertical heterostructures with other micropatterned electronic colloids, such as CNTs. We demonstrate a number of different devices and finally show that these a-PEDOT:PSS microstructures can be used in cell cultures to enable bioelectronics.

2. Result and discussion

2.1. PEDOT microgels

PEDOT:PSS is one of the most widely used organic electronic materials, thanks to its high conductivity and stability.[13] By tuning the doping level and morphology, the conductivity of PEDOT:PSS can be varied from semiconducting to metallic.[14] As an electroactive material, PEDOT:PSS is stable in both *in vivo* and *in vitro*. Commercially, high-conductivity PEDOT:PSS is available as a dispersion of particles with diameters of around 20 nm.[15] This fine dispersion passes through filtration membranes.[16] To pattern PEDOT:PSS into electronic devices, *in situ* gelation using cross-linking reagents[17,18] or pre-patterning of the oxidizer layer is used.[19] On the other hand, PEDOT:PSS is a polyelectrolyte complex, in which positively charged PEDOT is charge compensated and stabilized by negatively charged PSS. Divalent cations, such as copper(II)[17] and magnesium(II),[20] can induce the gel formation of PEDOT:PSS by cross-linking of PSS^-. Previously, it was found that sulfuric acid increases the doping level of PEDOT:PSS, accompanied by the release of a portion of the free PSS from the PEDOT:PSS complex and the reorganization of PEDOT regions.[21] Here, we studied this phenomenon more systematically by using the *in situ* rheology measurement during the acidification of PEDOT:PSS (see Experimental section for details). Fig. 1A shows rapid gelation with an initial locking within 2–3 minutes followed by a long term and slow consolidation which did not reach an equilibrium within 30 minutes of the measurement. The gelation is concentration dependent because a rubbery gel is formed in 1 M sulfuric acid, whereas a viscous non-Newtonian liquid is formed in 0.1 M sulfuric acid. Fig. 1B provides further insights into this dynamic behavior and clearly shows the rubbery plateau and the gel behavior in the case of 1 M sulfuric acid and a shear thickening viscous liquid in the case of 0.1 M sulfuric acid. The reference, as received, PEDOT:PSS dispersion has a behavior closer to that of a Newtonian liquid. We observed yield strain values of 60% and 20% for 0.1 and 1 M sulfuric acid, respectively.

Fig. 1C illustrates the gelling properties. When a droplet of 1 M sulfuric acid is placed next to a droplet of PEDOT:PSS, a blue a-PEDOT:PSS gel is immediately formed at the border of the two droplets.

To fabricate suspended microgel particles, large millimeter-sized blocks of aggregates (see Fig. 1D) were first formed *via* acidification. These flakes were collected by centrifugation, which also removed the excessive acid in the supernatant. Finally, a-PEDOT:PSS microgels were generated by vigorously stirring the collected aggregate gel dispersion in water (see schematic Fig. 1F). The a-PEDOT:PSS microgels were colloidally stable in water without visible precipitation for a minimum of two weeks. The acidification and re-dispersion resulted in microgel particle sizes in the scale of several micrometers (as visible from micrographs in Fig. 1E, and more detailed from the AFM phase images in Fig. S1, ESI†) so that they could be rapidly dewatered and retained on filtration membranes for micropatterning.

2.2. Tuning stability and conductivity with post-treatments

Many solvents, for example, dimethyl sulfoxide and diethylene glycol, induced phase separation between PEDOT and PSS and therefore enhanced the connectivity and conductivity of PEDOT:PSS.[22] We hypothesized that this treatment could also promote the interaction between PEDOT segments, creating a water-stable, cross-linked network. We chose methanol because it has a low boiling point and therefore evaporates quickly when added on top of the patterned a-PEDOT:PSS.[23] AFM images showed a distinct difference in surface morphologies between a-PEDOT:PSS and methanol-treated PEDOT:PSS films (Fig. S1A, ESI†). We formed a film using the a-PEDOT:PSS microgels and recorded a sheet resistance of 605 ± 76 Ω sq^{-1}. Rinsing with methanol decreased the sheet resistance of patterned structures to 232 ± 63 Ω sq^{-1} (Fig. S1B, ESI†). Then, we immersed the films into water and without methanol treatment, the a-PEDOT:PSS film quickly swelled, delaminated from the substrate, and disintegrated. However, the methanol-treated films showed superior stability in water. After 3 hours in water, the sheet resistance slightly increased to 251 ± 63 Ω sq^{-1} without any observable degradation or cracking of the films.

2.3. Micropatterning of a-PEDOT:PSS using printing and characterization of basic properties

We used the a-PEDOT:PSS microgels for micropatterning electronic structures as shown schematically in Fig. 2A and B.

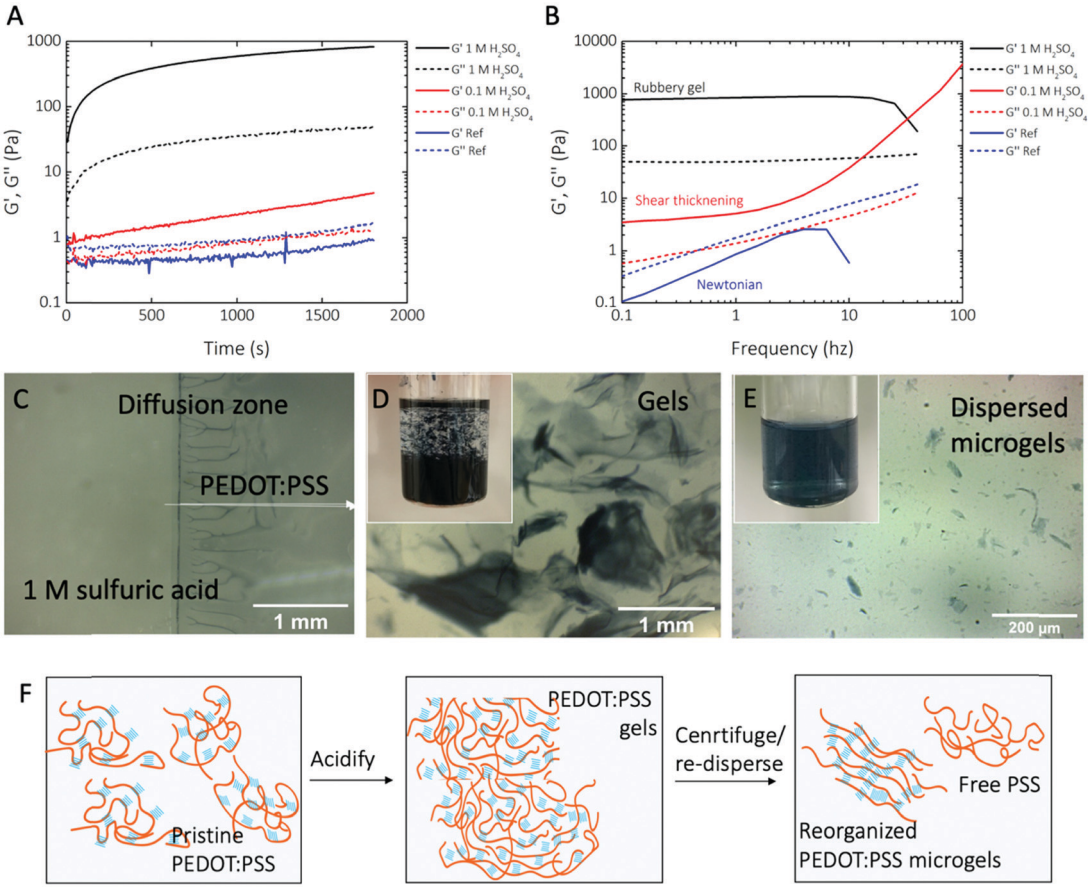

Fig. 1 Acidified PEDOT:PSS for patterning. (A) Rheology data showing the storage modulus (G') and loss modulus (G'') as a function of time after gel initiation by sulfuric acid. (B) Rheology data showing the storage modulus and loss modulus at different frequencies of the oscillator. Black and red lines represent PEDOT:PSS in different acid concentrations, and the blue line is PEDOT:PSS in water. (C) An interface between droplets of 1 M sulfuric acid and PEDOT:PSS showing the formation of the aggregates during sulfuric acid diffusion into PEDOT:PSS, which induced the gelation of PEDOT:PSS. (D) An optical micrograph showing the large flakes of the a-PEDOT:PSS gel. The inset is the image of the aggregated a-PEDOT:PSS flakes floating in water. (E) An optical micrograph showing the re-dispersed a-PEDOT:PSS microgel. The inset is the image of the microgels suspended in water. (F) Schematic of the proposed process during PEDOT:PSS acidification and dispersion.

Briefly, we used printed wax patterns onto PVDF membranes (a pore size of 0.45 or 0.25 μm). The versatility of wax printing allowed us to print arbitrary shapes with a precision of around 100 μm. Next, we micropatterned the aqueous dispersion of the a-PEDOT:PSS microgels by filtration through the membrane. The hydrophobic wax layer repels dispersed particles, forming patterns on the hydrophilic parts of the membrane. By controlling the amount of liquid and the concentration that passes through the filter membrane per wax-free area, as all a-PEDOT:PSS microgels remain in the filter, it is possible to control the final thickness and thus the sheet resistance of the patterned a-PEDOT:PSS layer (Fig. S1B, ESI†). We subsequently transferred the patterns from the membrane by pasting and peeling with an adhesive tape. These thin micropatterned a-PEDOT:PSS films were intrinsically flexible and could sustain mechanical deformations during peeling.

To analyze the resolution of filtration-assisted micropatterning of a-PEDOT:PSS, we formed thin line shapes with various widths and gaps. As shown in Fig. 2C, the minimal line resolution achieved was around 100 μm, which was due to limitations of the wax printer and not the filtration-assisted patterning technique. Due to the structure of the microgels, the filtration patterned a-PEDOT:PSS showed fuzzy and rough edges. However, a minimal gap distance of 100 μm was still achievable. Both the line and the gap could be reliably patterned at a resolution of 200 μm. This resolution was in line with that reported for MXenes[8] or metal nanowires,[9] using the same patterning technique, and was sufficiently high for many of device fabrications, for example in wearable electronics and analytical applications.[24]

Additionally, the gel properties of a-PEDOT:PSS allow the patterned a-PEDOT:PSS films to heal upon rewetting. (Fig. S2 and S3, ESI†).

The a-PEDOT:PSS pattern forms an electrochemical active surface that is accessible to ions. To estimate its surface area, we patterned barbell electrodes and measured their electrochemical surface areas from CVs using Randles–Sevick equation (Fig. S4, ESI†). For a geometric area of 7 mm^2, we estimated an electrochemical surface area of 32 ± 2 mm^2, suggesting that the microgel network provides a significant amount of electroactive sites in its bulk.[25] This observation is also in accordance with the

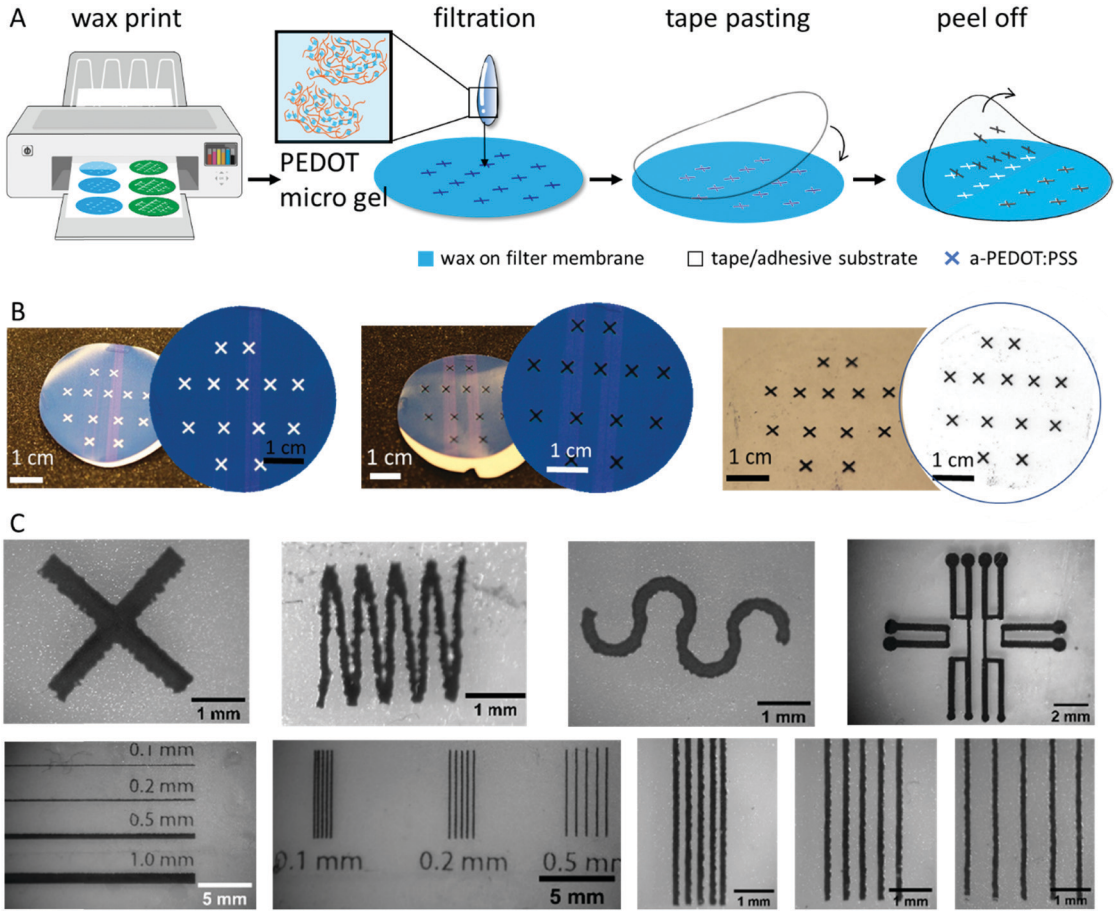

Fig. 2 (A) Schematics of the filtration-assisted patterning of a-PEDOT:PSS microgels. (B) Images of the different stages of patterning, from left to right: (1) the wax-patterned filtration membrane, (2) a-PEDOT:PSS on the membrane, and (3) a-PEDOT:PSS patterns transferred onto the transparent tape. The right side of each panel is the scanned image. (C) Optical micrographs of the representative patterned a-PEDOT:PSS: cross, zig-zag and serpentine shapes, the optical micrograph of arrays of a-PEDOT:PSS channels, the resolution test of a-PEDOT:PSS with lines of various sizes with the thinnest line is 100 μm – note that the letters were also patterned in a-PEDOT:PSS – and the resolution test showing the minimal gap distance between each line of 200 μm.

high surface area typically reported for PEDOT:PSS-modified metal substrates.[26]

2.4. Heterostructures

With a-PEDOT:PSS as the active material and assisted by the peel-and-transfer method, we show that the method can be used to pattern microscale devices with multilayered heterostructures. For this purpose, we also patterned single-walled CNT dispersed in water using the same method. Fig. 3A shows the schematics of the general approach for the fabrication of heterostructures: we patterned CNT electrodes and transferred these patterns from the filter membrane onto the tape which was pre-patterned with a-PEDOT:PSS microstructures (as described in Section 2.3) to form multilayers, as shown in Fig. 3B and C. After methanol treatment, a-PEDOT:PSS and CNT channels formed a compact electronic contact with each other as shown in Fig. 3D and E. Therefore, we could use CNTs as electrodes to contact a-PEDOT:PSS, and this is useful in many devices including transistors. We could measure the resistance of a "cross" shaped a-PEDOT:PSS between two CNT electrodes to 1200 Ω after methanol treatment.

2.5. Micropatterned multilayer organic electrochemical transistors (OECTs) and supercapacitors

The patterning method allowed interdigitated electrodes, which is a useful geometry, to be patterned (see schematic Fig. 4A) for micro supercapacitors and electroanalytical micro devices, at a resolution of 200 μm without defects and shorts (Fig. 4B). Higher resolution is also achievable, although increasing the risk of creating shorts when the gap between the interdigitated a-PEDOT:PSS electrodes is decreased. We casted a 1 M aqueous NaCl solution onto the interdigitated methanol-treated a-PEDOT:PSS electrodes as the electrolyte to create a planar micro supercapacitor. The CVs of the device at different scan rates are shown in Fig. 4C, and charge/discharge curves are shown in Fig. 4D. At a scan rate of 2 mV s^{-1}, we achieved a specific capacitance of 1.6 mC cm^{-2}. It should be noted that this number is on the lower end of PEDOT:PSS supercapacitors compared with previously reported capacitors due to the relatively low conductivity of PEDOT:PSS itself as both the active material and the current collector.[27]

To demonstrate more advanced devices, we fabricated organic electrochemical transistors (OECTs). These are based on the semiconducting, electrochemically active properties of PEDOT:PSS,

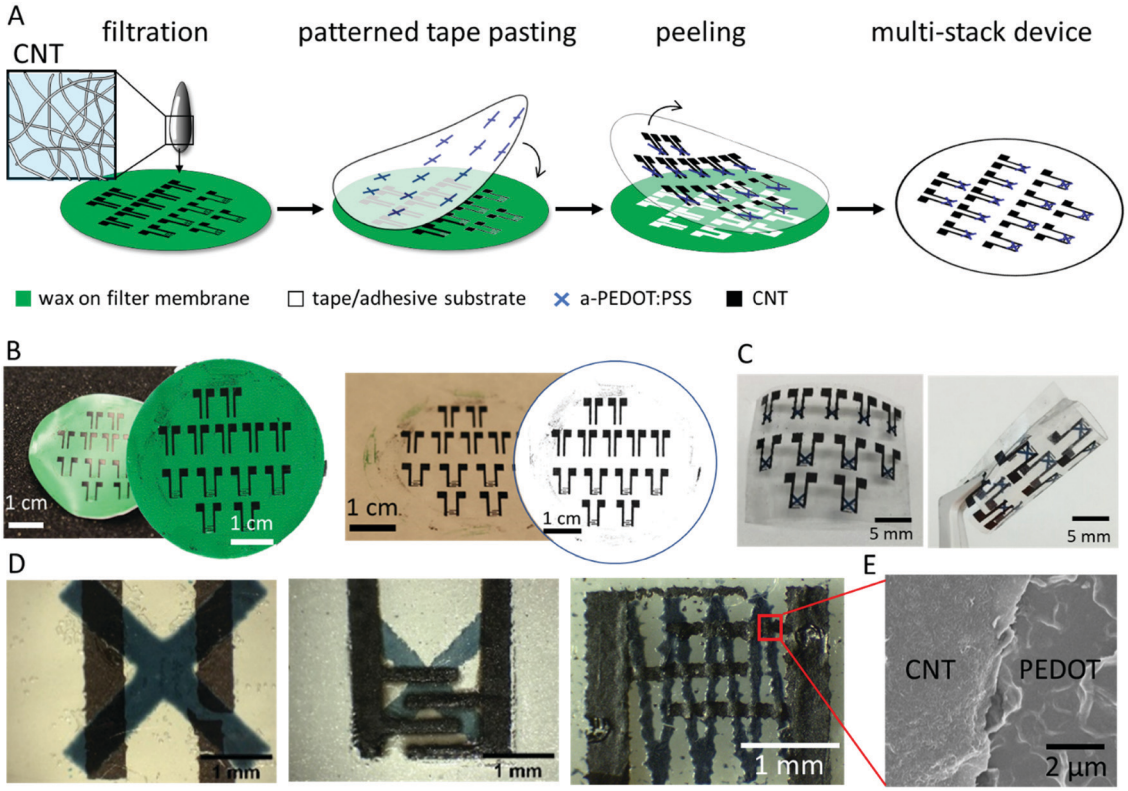

Fig. 3 (A) Schematics of the filtration-assisted patterning of carbon nanotubes (CNTs), from dispersion, and the fabrication of multi-stack, heterogeneous devices by joining these patterns with a-PEDOT:PSS patterns. (B) Images of the CNT patterns on the wax-patterned filtration membrane (left) and the CNT patterns transferred onto the transparent tape (right). The right side of each panel is the scanned image of the sample. (C) Image of a 2-layer device with a-PEDOT:PSS and CNT micropatterns. (D) Images of a 2-layer transistor arrays with methanol-treated CNTs as electrodes and a-PEDOT:PSS "cross" or "serpentine" shapes as the channel on a flexible substrate. (E) SEM image of the cross section between a-PEDOT:PSS and CNT in a 2-layer stacked device after methanol treatment.

where the doping level of PEDOT is modulated by a gate electrode soaked in an electrolyte.[28] We fabricated OECTs by patterning the multiplexed a-PEDOT:PSS gate adjacent to the a-PEDOT:PSS channel, as shown schematically in Fig. 4E and micrographically in Fig. 4F. Using the patterned PEDOT, we fabricated four transistor gates next to four independent channels. The distance between the gate and the channel was ~2 mm, and the channel length was ~1 mm. In this design, the gates shared a common contact, where they were transferred onto the device layer after assembling the device. It is also possible to pattern the channels and gates first on the same layer, followed by transferring CNT contacts onto the layer to complete the device. The gate and channels were connected by drop-casting 1 M NaCl electrolyte onto them. Fig. 4G shows the performance of a representative channel. At a gate voltage of −0.2 V, the a-PEDOT:PSS channel oxidized (doped) and showed a high current of over −0.2 mA at a drain-to-source voltage (VDS) of −0.6 V. The drain-to-source current (IDS) decreased as the gate voltage moved to the positive region due to the reduction (dedoping) of the a-PEDOT:PSS channel. At a gate voltage of around 0.5 V, the channel was turned off, with an on/off ratio of around 20 (Fig. 4H). The relatively large channel thickness and dimension, the low conductivity of CNT contacts as compared with the commonly used gold contacts, and the electrochemical oxidation at the channel at a higher VDS, contribute to the lowering of the on/off ratio compared with the state of the art OECTs,[2] but still suffice especially for biological applications where transconductance is more important than the on/off ratio. The methanol-treated a-PEDOT:PSS OECT devices also showed high stability in the aqueous electrolyte. We cycled the device with a switching on/off time of around ~1 s, and after 300 cycles, the device retained 90% of its initial IDS as shown in Fig. 4I and J.

We also fabricated three- and four-layer devices by sandwiching the electrolyte between the OECT and the gate. First, we patterned the CNT finger electrodes with a distance of ~500 μm as the channel length onto the PEDOT:PSS cross pattern. We used a polymer membrane, poly(acrylic acid)/poly(ethylene oxide) (PAA/PEO), as the solid electrolyte. In its dry state, PAA/PEO is a free-standing, transparent membrane that can be directly superimposed onto the methanol-treated a-PEDOT:PSS/CNT pattern, as shown schematically in Fig. 4K. The mechanical properties of PAA/PEO allowed for the a-PEDOT:PSS gate layer to be pasted from the filter membrane onto the PAA/PEO membrane (Fig. 4L and M). We showed that upon hydration of the PAA/PEO separator/electrolyte membrane, the OECT could be modulated with the a-PEDOT:PSS gate (Fig. 4N and O).

2.6. Biocompatibility

An important application area for advanced organic electronic devices is the field of bioelectronics *in vivo* and *in vitro*. To demonstrate that our devices are biocompatible, we used

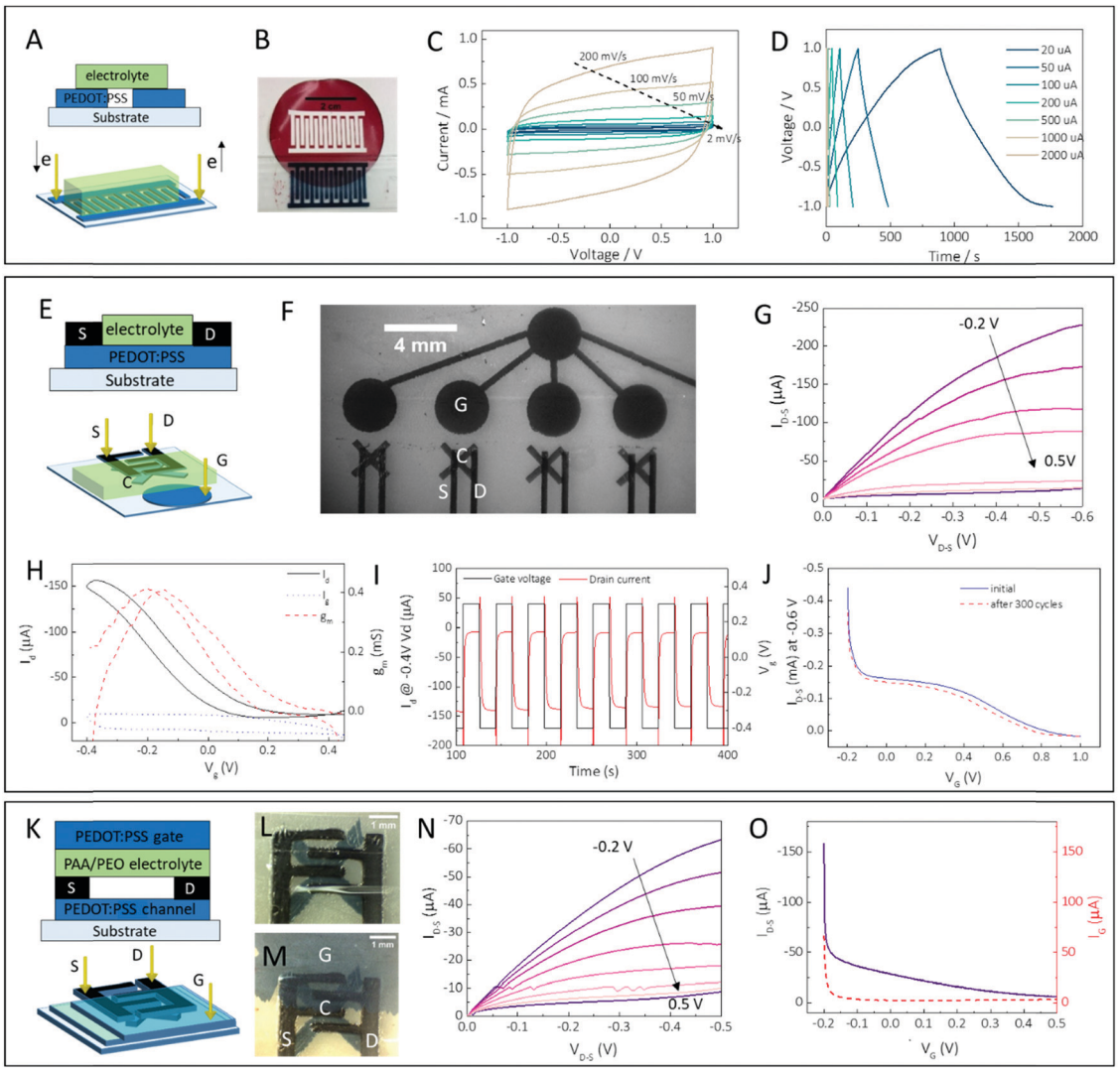

Fig. 4 Heterostructures of methanol-treated a-PEDOT:PSS devices. (A) Two-layer structure of the interdigitated supercapacitor. (B) Image of the wax-patterned filtration membrane and the transferred a-PEDOT:PSS supercapacitor. (C) CVs of the device as shown in B at different scan rates. The electrolyte was 1 M NaCl. (D) Charge–discharge curves of device B. (E) Schematics of the three-layer structure transistors indicating source *S*, drain *D*, channel *C* and gate *G*. (F) The a-PEDOT:PSS transistor array with a multiplexed electrode. The image shows 4 channels. (G) Steady-state parameters of a transistor shown in (F). The electrolyte was PBS in the agarose gel. (H) Transfer curve at VDS = −0.4 V of an a-PEDOT:PSS device showing hysteresis during sweeping. (I) Switching profile of the device in (F). The drain voltage was set at −0.4 V and the gate voltage was switched between −0.4 V and +0.3 V. (J) Transfer curve of the device before and after 300 cycles of switching at VDS = −0.6 V. (K) Schematics of the four-layer structure of an a-PEDOT:PSS transistor, with the gate layer placed vertically to the channel, separated by an electrolyte membrane. (L) Optical micrograph of the transistor with an electrolyte membrane directly placed on top. (M) Optical micrograph of the same device in (L), with the a-PEDOT:PSS gate transferred on top of the separator membrane. (N) Steady-state parameters of the device in M. (O) Transfer curve of the device at VDS = −0.4 V. The dotted line is the gate current. The electrolyte is 1 M NaCl.

human tumor-derived glioblastoma U87 cells and Lund Human Mescencephalic (LUHMES) neuronal cells and cultivated them on the micropatterned methanol-treated a-PEDOT:PSS electrodes, similar to the pattern shown in Fig. 2C (right). These micropatterned a-PEDOT:PSS films were transferred onto a medical tape, treated with methanol and enclosed in a polydimethylsiloxane (PDMS) well for seeding the cells (Fig. 5A). The medical tape was used as a substrate when involving cell cultivation due to its reported compatibility with other cell culture models and minimal cytotoxicity compared with the conventional scotch tape.[29]

We grew U87 and LUHMES cells on top of the a-PEDOT:PSS electrodes and the tape (Fig. 5C–F and Fig. S5, ESI†). Cell counting showed that the U87 cells continued to proliferate as their number increased compared to the seeded density of 20 000 cells per cm^2 (Fig. 5G). The U87 cells proliferate at a similar rate on a-PEDOT:PSS and on the tape between two electrodes in comparison with cells growing in conventional well plates or on the tape without patterned a-PEDOT:PSS electrodes. A similar cell behavior on the different surfaces was also observed when comparing the total surface area covered by the U87 cells (Fig. 5H).

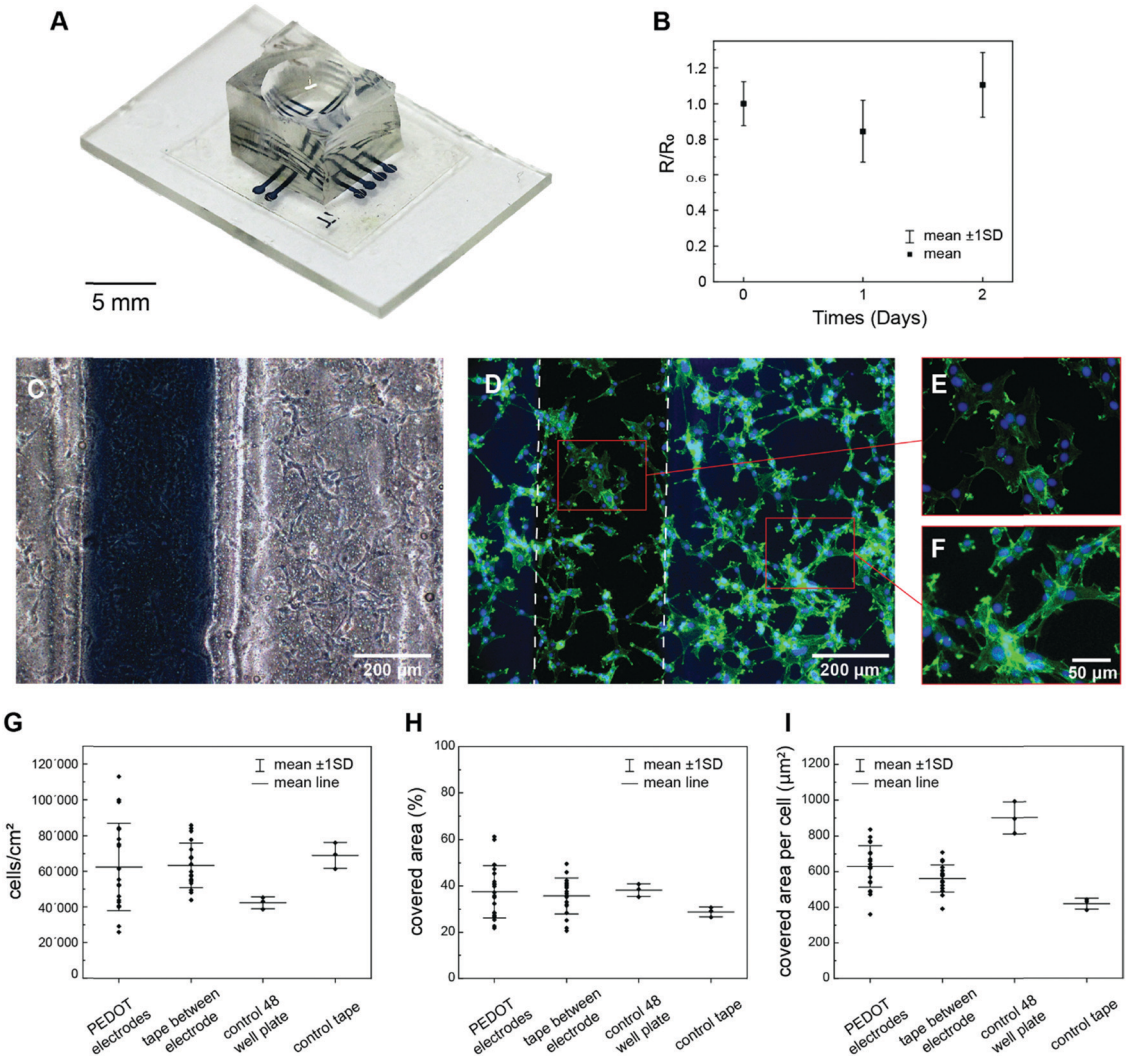

Fig. 5 U87 cells cultivated for 2 days on a-PEDOT:PSS electrodes and on the tape. (A) Image of the cell culture. (B) Change in resistance of the a-PEDOT:PSS micropatterns as a function of time while being immersed in the cell culture. (C) Bright field image and (D) fluorescence image stained with phalloidin (green) and Hoechst (blue). (E and F) Zoomed-in images of cells growing on a-PEDOT:PSS and on the tape, respectively. (G) Counted number of cells per cm^2, (H) cell coverage in percentage and (I) average cell coverage of a single cell on the a-PEDOT:PSS, tape, conventional 48-well plate and on tape without patterned electrodes as the control.

The average area that a single cell covers on a-PEDOT:PSS and on the tape was slightly lower than that observed in the conventional well plate (Fig. 5I). We hypothesized that this is due to the difference in surface roughness and softness of PEDOT:PSS and the tape compared with the well plates made of polystyrene. The sheet resistance of the electrodes increased slightly from $21.7 \pm 1.3\ \Omega\ sq^{-1}$ to $24.1 \pm 2.5\ \Omega\ sq^{-1}$ after being submerged in the cell culture media and incubated at 37 °C for two days (Fig. 5B), demonstrating that the micropatterned electrodes could function *in vitro*.

The analysis with the U87 cells not only shows that the cells survive on the electrodes and the medical tape, but also show a similar growth behavior to that in the conventional cell culture well plates. This is essential when addressing biological questions for *in vitro* cell culture model studies. The compatibility of the described patterned a-PEDOT:PSS electrodes with U87 and LUHMES cells gives opportunities, for example, for recording the electrophysiological cell signals using a-PEDOT:PSS-based OECTs.

3. Conclusion

In conclusion, we have developed an acidified PEDOT:PSS microgel that can be easily micropatterned using simple techniques such as wax printing, filtration, and adhesive tape method. This method can pattern PEDOT films into arbitrary geometries with a resolution reaching 100 µm. These micropatterns have further been rendered water resilient using post-methanol treatment. Using CNTs as other types of electroactive materials dispersed in water, we can build vertically stacked, heterostructure microelectronic devices through peeling-and-

pasting different micropatterned materials. We show that this method can rapidly prototype numerous advanced microelectronic structures and devices including electrodes, micro supercapacitors and organic electrochemical transistors with up to four layers of different materials. The time and cost-efficient fabrication of stable multilayer devices is a unique property of this method compared with previously described PEDOT:PSS patterning methods (see Table S1, ESI†). Finally, we showed that the acidified PEDOT:PSS micropatterns were compatible with human U87 and LUHMES cell cultures, which enable the use of this technique for bioelectronic devices.

This method can be used with many other colloidal materials such as graphene and other 2D materials or cellulose/protein nanofibrils, and enables rapid prototyping of a plethora of multilayer microelectronic devices and applications ranging from printed electronics[30] to *in vivo* bioelectronics for drug delivery[31] or neural contacts[24,32] and *in vitro* electrode interfaces for mammalian cells and bacterial cultures[2] or for epidermal electronics.[33,34]

4. Materials and methods

4.1. Materials

PEDOT:PSS (Clevios PH1000) was purchased from Heraeus. Multiwall and single wall carbon nanotube (MWCNT and SWCNT) dispersions were prepared as described in ref. 34. Poly(acrylic acid)/poly(ethylene oxide) (PAA/PEO) membranes were assembled using the layer-by-layer assembly method described in ref. 35. Durapore PVDF (0.45 μm) membrane filters were purchased from Sigma-Aldrich. Growth factor-reduced Matrigel was purchased from Corning. Advanced DMEM, N-2, L-glutamine, BSA, Alexa Fluor 488 Phalloidin and Hoechst were purchased from Thermo Fischer. Fibroblast growth factor and GDNF were purchased from R&D Systems. Dibutyryl cAMP was purchased from Selleckchem. All the other chemicals were purchased from Sigma-Aldrich and were used without further purification.

4.2. Rheology measurements

Rheology measurements of a-PEDOT:PSS hydrogels were carried out using a DHR-2 rheometer (TA Instruments, USA) with a 25 mm diameter parallel plate geometry with a gap of 500 μm. A Peltier plate was used to maintain the temperature at 25 °C. The procedure was started by adding 0.3 mL of the PEDOT:PSS suspension with a concentration of 1.3 wt% to the Peltier plate and the top plate was lowered to the gap so that the volume between the plates were filled by the suspension. 0.3 mL of sulfuric acid of different concentrations was slowly and evenly added along the circumference to initiate the gelling process, and a time sweep measurement (0.5% strain at 1 Hz) was initiated to track the kinetics of the gelling for the first 30 minutes. The gelling was not at a steady state after 30 min, but at longer times drying of the gel was observed. The time sweep was immediately followed by a frequency (0.025% strain at 0.1–100 Hz) and an Amplitude sweep (0.1–100% strain at 1 Hz).

4.3. Preparation of the acidified PEDOT:PSS (a-PEDOT:PSS)

To a vial containing 10 mL of PEDOT:PSS, 10 mL of 1 M sulfuric acid aqueous solution was added dropwise with constant stirring. The blue precipitate was collected by centrifuging at 4500 rpm for 15 minutes. 100 mL of de-ionized water was added to the pellet. The whole mixture was dispersed by vigorous stirring at 1500 rpm overnight. The resultant dispersion of a-PEDOT:PSS was stable under room conditions. Too gentle stirring results in a larger particle size of the gel dispersion and minimizes the quality and resolution of the wax printing-assisted filtration.

4.4. Wax printing-assisted filtration patterning

All the patterns were drawn using Adobe Illustrator and directly printed onto hydrophilic PVDF membranes. The membrane was hydrated before adding the materials. The stock solution of the colloids, including a-PEDOT:PSS (0.1 wt%) and CNT (1 g L^{-1}), was diluted by at least 10 times before being filtered through the membrane. The materials were retained at the hydrophilic regions of the membrane. After drying, the patterns can be either directly peeled off, transferred onto scotch tapes or onto a pre-patterned tape to create heterostructure multi-stack layers.

4.5. Characterization

Optical image analysis was performed using Fiji. AFM images were collected under ambient conditions using a MultiMode 8 (Bruker, Santa Barbara, CA, USA) setup in the SCANASYST mode with a SCANASYST-AIR cantilever.

4.6. Cell cultivation

To cultivate cells on a-PEDOT:PSS electrodes, a simple customized PDMS (Sylgard 184)-based well set up was used. PDMS and curing agent were mixed at a weight ratio of 10 : 1, poured into a Petri dish, degassed and hardened at 70 °C overnight. The PDMS wells were cut using a 6 mm biopsy punch and placed on the medical tape (3 M, 9877) which had been patterned with methanol-treated a-PEDOT:PSS electrodes. Prior to cell seeding, the devices were soaked in 70% ethanol for 5 minutes, washed 3 times with PBS and coated with the attachment factor protein by incubating for 30 minutes for U87 cells (ATCC) or growth factor-reduced Matrigel (1 : 100) for LUHMES cells (abm) for 4 hours at 37 °C. The U87 cells were seeded at 20 000 cells per cm^2 and were cultivated in DMEM/10% FBS/1%PS for 2 days. The LUHMES cells were cultivated following the protocol described by Sholz *et al.*[36] For proliferation, the cells were kept in Advanced DMEM/F12, 1x N-2 supplement, 2 mM L-glutamine and 40 ng mL^{-1} fibroblast growth factor. Differentiation media consisted of advanced DMEM/F12, 1x N-2 supplement, 2 mM L-glutamine, 1 mM dibutyryl cAMP, 1 μg mL^{-1} tetracycline and 2 ng mL^{-1} human GDNF. To differentiate LUHMES, the cells were seeded into a T25 flask with proliferation media and after 24 hours, the media were changed to differentiation media for 2 days. The cells were then reseeded onto the patterned a-PEDOT:PSS electrodes at a density of

150 000 cells per cm^2. For staining, the cells were fixed in 4% methanol-free formaldehyde solution for 15 minutes at RT and washed 3 times with PBS. The samples were incubated in PBS/0.1% Triton $X-100$ for 15 minutes at RT before staining with Hoechst (1 : 2000) in PBS for 10 minutes followed by Alexa Fluor 488 Phalloidin (1.65 μM) for 1 hour at RT and washed again 2 times with PBS. Images were acquired using a fluorescence microscope Nikon eclipse Ti–S and an Infinity 2 camera from Lumenera. Image analysis was performed using Fiji.

Author contributions

LO and SB contributed equally to this work. LO and MH devised this project and wrote the manuscript. LO performed the experiments. CM measured the OECT performances. ZH prepared the electrolytes and membranes. SB and AH performed the biological tests and edited the manuscript with LO and MH. WT facilitated the filtration process. SK helped to develop the device patterning method. HL conducted the AFM measurements. T. B. performed the rheology measurement and analysis. All the authors have contributed to manuscript writing. The manuscript was written through contributions of all the authors. All the authors have given approval to the final version of the manuscript.

Conflicts of interest

The authors declare no conflicts of interest.

Acknowledgements

M. M. H. and L. O. acknowledge the European Research Council (Grant 715268), Z. W. acknowledges the Wenner-Gren Foundation, S. B. acknowledges Vetenskapsrådet, and W. T. and A. H. acknowledge the Wallenberg Foundation.

References

1 C. Müller, L. Ouyang, A. Lund, K. Moth-Poulsen and M. M. Hamedi, *Adv. Mater.*, 2019, **31**, 1807286.
2 E. Zeglio, A. L. Rutz, T. E. Winkler, G. G. Malliaras and A. Herland, *Adv. Mater.*, 2019, **31**, 1806712.
3 S. Middya, V. F. Curto, A. Fernández-Villegas, M. Robbins, J. Gurke, E. J. Moonen, G. S. Kaminski Schierle and G. G. Malliaras, *Adv. Sci.*, 2021, 2004434.
4 L. D. Garma, L. M. Ferrari, P. Scognamiglio, F. Greco and F. Santoro, *Lab Chip*, 2019, **19**, 3776–3786.
5 S. K. Sinha, Y. Noh, N. Reljin, G. M. Treich, S. Hajeb-Mohammadalipour, Y. Guo, K. H. Chon and G. A. Sotzing, *ACS Appl. Mater. Interfaces*, 2017, **9**, 37524–37528.
6 H. Yuk, B. Lu, S. Lin, K. Qu, J. Xu, J. Luo and X. Zhao, *Nat. Commun.*, 2020, **11**, 1604.
7 M. M. Hamedi, A. Ainla, F. Güder, D. C. Christodouleas, M. T. Fernández-Abedul and G. M. Whitesides, *Adv. Mater.*, 2016, **28**, 5054–5063.
8 W. Tian, A. VahidMohammadi, M. S. Reid, Z. Wang, L. Ouyang, J. Erlandsson, T. Pettersson, L. Wågberg, M. Beidaghi and M. M. Hamedi, *Adv. Mater.*, 2019, **31**, 1902977.
9 K. Tybrandt and J. Vörös, *Small*, 2016, **12**, 180–184.
10 K. Tybrandt, D. Khodagholy, B. Dielacher, F. Stauffer, A. F. Renz, G. Buzsáki and J. Vörös, *Adv. Mater.*, 2018, **30**, 1706520.
11 A. Hajian, Z. Wang, L. A. Berglund and M. M. Hamedi, *Adv. Electron. Mater.*, 2019, **5**, 1800924.
12 S.-M. Kim, N. Kim, Y. Kim, M.-S. Baik, M. Yoo, D. Kim, W.-J. Lee, D.-H. Kang, S. Kim, K. Lee and M.-H. Yoon, *NPG Asia Mater.*, 2018, **10**, 255–265.
13 G. Dijk, A. L. Rutz and G. G. Malliaras, *Adv. Mater. Technol.*, 2020, **5**, 1900662.
14 O. Bubnova, Z. U. Khan, A. Malti, S. Braun, M. Fahlman, M. Berggren and X. Crispin, *Nat. Mater.*, 2011, **10**, 429–433.
15 W. Lövenich, *Polym. Sci., Ser. C*, 2014, **56**, 135–143.
16 S. Kim, B. Sanyoto, W.-T. Park, S. Kim, S. Mandal, J.-C. Lim, Y.-Y. Noh and J.-H. Kim, *Adv. Mater.*, 2016, **28**, 10149–10154.
17 V. R. Feig, H. Tran, M. Lee, K. Liu, Z. Huang, L. Beker, D. G. Mackanic and Z. Bao, *Adv. Mater.*, 2019, **31**, 1902869.
18 B. Lu, H. Yuk, S. Lin, N. Jian, K. Qu, J. Xu and X. Zhao, *Nat. Commun.*, 2019, **10**, 1–10.
19 J. Edberg, D. Iandolo, R. Brooke, X. Liu, C. Musumeci, J. W. Andreasen, D. T. Simon, D. Evans, I. Engquist and M. Berggren, *Adv. Funct. Mater.*, 2016, **26**, 6950–6960.
20 S. Ghosh and O. Inganäs, *Adv. Mater.*, 1999, **11**, 1214–1218.
21 Z. Li, H. Sun, C.-L. Hsiao, Y. Yao, Y. Xiao, M. Shahi, Y. Jin, A. Cruce, X. Liu, Y. Jiang, W. Meng, F. Qin, T. Ederth, S. Fabiano, W. M. Chen, X. Lu, J. Birch, J. W. Brill, Y. Zhou, X. Crispin and F. Zhang, *Adv. Electron. Mater.*, 2018, **4**, 1700496.
22 L. Ouyang, C. Musumeci, M. J. Jafari, T. Ederth and O. Inganäs, *ACS Appl. Mater. Interfaces*, 2015, **7**, 19764–19773.
23 D. Alemu, H.-Y. Wei, K.-C. Ho and C.-W. Chu, *Energy Environ. Sci.*, 2012, **5**, 9662–9671.
24 D. Gao, K. Parida and P. S. Lee, *Adv. Funct. Mater.*, 2019, 1907184.
25 K. Wijeratne, U. Ail, R. Brooke, M. Vagin, X. Liu, M. Fahlman and X. Crispin, *Proc. Natl. Acad. Sci. U. S. A.*, 2018, **115**, 11899–11904.
26 X. Cui and D. C. Martin, *Sens. Actuators, B*, 2003, **89**, 92–102.
27 A. V. Volkov, K. Wijeratne, E. Mitraka, U. Ail, D. Zhao, K. Tybrandt, J. W. Andreasen, M. Berggren, X. Crispin and I. V. Zozoulenko, *Adv. Funct. Mater.*, 2017, **27**, 1700329.
28 J. Rivnay, S. Inal, A. Salleo, R. M. Owens, M. Berggren and G. G. Malliaras, *Nat. Rev. Mater.*, 2018, **3**, 1–14.
29 T. E. Winkler, M. Feil, E. F. Stronkman, I. Matthiesen and A. Herland, *Lab Chip*, 2020, **20**, 1212–1226.
30 H. Li and J. Liang, *Adv. Mater.*, 2019, 1805864.
31 M. R. Abidian and D. C. Martin, *Biomedical Applications of Electroactive Polymer Actuators*, 2009, p. 279.
32 R. Green and M. R. Abidian, *Adv. Mater.*, 2015, **27**, 7620–7637.

33 D.-H. Kim, N. Lu, R. Ma, Y.-S. Kim, R.-H. Kim, S. Wang, J. Wu, S. M. Won, H. Tao and A. Islam, *Science*, 2011, **333**, 838–843.
34 Z. Wang, L. Ouyang, W. Tian, J. Erlandsson, A. Marais, K. Tybrandt, L. Wågberg and M. M. Hamedi, *Langmuir*, 2019, **35**, 10367–10373.
35 Z. Wang, L. Ouyang, H. Li, L. Wågberg and M. M. Hamedi, *Small*, 2021, **17**, 2100954.
36 D. Scholz, D. Pöltl, A. Genewsky, M. Weng, T. Waldmann, S. Schildknecht and M. Leist, *J. Neurochem.*, 2011, **119**, 957–971.